

Percutaneous pulmonary valve replacement using completely tissue-engineered off-the-shelf heart valves: six-month *in vivo* functionality and matrix remodelling in sheep



Boris Schmitt^{1*}, MD; Hendrik Spriestersbach¹, MD; Darach O h-Icí¹, MD; Torben Radtke¹; Marco Bartosch¹, Dipl. Ing.; Heiner Peters¹, Dipl. Ing.; Matthias Sigler², MD, PhD; Laura Frese³, PhD; Petra E. Dijkman³, PhD; Frank P. T. Baaijens⁴, PhD; Simon P. Hoerstrup³, MD, PhD; Felix Berger¹, MD, PhD

1. Department of Congenital Heart Disease and Paediatric Cardiology, Deutsches Herzzentrum Berlin, Berlin, Germany; 2. Department of Paediatric Cardiology and Paediatric Intensive Care Medicine, Georg-August University, Göttingen, Germany; 3. Division of Surgical Research, University and University Hospital Zürich, Zürich, Switzerland; 4. Department of Biomedical Engineering, Eindhoven University of Technology, Eindhoven, The Netherlands

This paper also includes supplementary data published online at: http://www.pcronline.com/eurointervention/98th_issue/12

B. Schmitt and H. Spriestersbach are joint first authors and contributed equally to this work.

S.P. Hoerstrup and F. Berger are joint last authors and contributed equally to this work.

KEYWORDS

- cardiac catheterisation
- heart valve
- heart valve prosthesis implantation
- percutaneous pulmonary valve replacement
- tissue engineering

Abstract

Aims: The objective was to implant a stented decellularised tissue-engineered heart valve (sdTEHV) percutaneously in an animal model, to assess its *in vivo* functionality and to examine the repopulation and remodelling of the valvular matrix by the recipient's autologous cells.

Methods and results: Prototypes of sdTEHV were cultured *in vitro*, decellularised and percutaneously implanted into the pulmonary position in 15 sheep. Functionality was assessed monthly by intracardiac echocardiography (ICE). Valves were explanted after eight, 16 or 24 weeks and analysed macroscopically, histologically and by electron microscopy. Implantation was successful in all animals. Valves showed normal pressure gradients throughout the study. Due to a suboptimal design with small coaptation area, stent ovality led to immediate regurgitation which continuously increased during follow-up. Analyses revealed complete endothelialisation and rapid cellular repopulation and remodelling of the entire matrix. Valves were free from endocarditis, calcification and graft rejection.

Conclusions: sdTEHV can be safely implanted percutaneously. The fast autologous recellularisation and the extensive matrix remodelling demonstrate the valve's potential as a next-generation percutaneous prosthesis with the capacity for tissue self-maintenance and longevity. Regurgitation may be prevented by valve design optimisation.

*Corresponding author: Department of Congenital Heart Disease and Paediatric Cardiology, Deutsches Herzzentrum Berlin, Augustenburger Platz 1, 13353 Berlin, Germany. E-mail: schmitt@dhzb.de

Abbreviations

CT	computed tomography
ECM	extracellular matrix
ICE	intracardiac echocardiography
PA	pulmonary artery
RVOT	right ventricular outflow tract
sdTEHV	stented decellularised tissue-engineered heart valve
SEM	scanning electron microscopy
SMA	smooth muscle actin

Introduction

Many congenital heart defects affect the pulmonary valve^{1,2}. Patients with such defects often undergo multiple interventions, as current valve prostheses are not durable enough to last a lifetime.

Surgical pulmonary valve replacement can be avoided in selected patients by implanting pulmonary valve prostheses percutaneously³. These prostheses are made from glutaraldehyde-fixed bovine tissue^{4,5}. They degrade with time, as the leaflet tissue cannot be maintained or renewed by the body⁶. A valve with regenerative capacity would overcome these limitations. Attempts to use *in vitro* tissue-engineered living heart valves failed in preclinical studies due to leaflet shortening caused by cell-mediated traction forces⁷⁻⁹.

An alternative approach uses decellularised *in vitro* tissue-engineered heart valves^{10,11}. Decellularisation prevents leaflet retraction by removing contractile cells, leaving the extracellular matrix (ECM) behind^{10,12}. Decellularisation substantially simplifies the process from valve production to implantation as valves are less immunogenic and can be stored. This makes it possible to produce the valve as a human cell-derived homologous off-the-shelf product¹⁰. Such valves have shown self-repair capacity in primates and sheep: they were swiftly populated with host cells and demonstrated matrix remodelling^{13,14}.

In these studies, the valves were integrated into self-expanding stents and implanted using a right ventricular transapical approach. As the next step towards human application, we developed a delivery system for percutaneous transvenous implantation¹⁵. We demonstrated the principal feasibility of replacing the pulmonary valve using our delivery system and sdTEHVs in three sheep.

Editorial, see page 11

In the study presented here, the focus was on the *in vivo* functionality and histologic results of sdTEHV up to six months after percutaneous implantation in the pulmonary position in a series of 15 sheep.

Methods

STUDY DESIGN

Approval for this animal experiment was given by the responsible body (Regional Office for Health and Social Affairs Berlin, LAGeSo). Animals were treated according to the guidelines of the European and German Societies of Laboratory Animal Science (FELASA, GV-SOLAS).

Fifteen adult grey horned heaths were randomly divided into three groups of five animals with a follow-up period of eight, 16 and 24 weeks. CT scans were performed before valve implantation, one week after implantation and one week before explantation.

Valve function was evaluated by intracardiac echocardiography (ICE) every four weeks. Anaesthesia and perioperative procedures have been described previously.

HEART VALVE FABRICATION AND IMPLANTATION PROCEDURE

The valves were produced from ovine vascular-derived cells seeded on a fast degrading polyglycolic acid scaffold coated with poly-4-hydroxy-butyrate and integrated into 30×30 mm nitinol stents (pfm medical ag, Cologne, Germany). After decellularisation and sterilisation they were stored at 4°C^{10,16} and implanted 8.5±5.9 weeks after manufacture. Production was carried out by XELTIS BV (Eindhoven, The Netherlands).

The implantation procedure has been described previously. Briefly, native pulmonary valve function was assessed by ICE. Angiography and pressure measurements were performed in the right atrium, ventricle and pulmonary artery. The sdTEHV was inspected and the leaflets were separated with a scalpel. The sdTEHV was crimped in a stepwise fashion to a minimal diameter of 8 or 10 mm using a crimping tool (Edwards Lifesciences, Irvine, CA, USA). The crimped sdTEHV was loaded into a custom-made delivery system¹⁵ with a shaft of 22 Fr (outer diameter) and a capsule at the distal end with an inner/outer diameter of either 8/8.6 mm (26 Fr) or 10/10.6 mm (32 Fr) (**Figure 1**). The size of the capsule was selected with respect to animal weight, jugular vein size and the individual crimpability of the sdTEHV.

The delivery system was inserted without a sheath into the jugular vein. In the ovine model the jugular access must be used, as – different from humans – the femoral veins are too small. The delivery system was advanced under fluoroscopic guidance to the pulmonary valve position over an ultra-stiff guidewire (Amplatz Ultra-Stiff Wire Guide, Ultra-Stiff 2, Curved – PTFE-Coated Stainless Steel; William Cook Europe, Bjaeverskov, Denmark). By withdrawing the capsule, the self-expanding sdTEHV was released, overstenting the native pulmonary valve. After implantation, the position and function of the sdTEHV were assessed using angiography, invasive pressure measurements and ICE (**Figure 2**). Anticoagulation was continued for five days using acetylsalicylic acid 100 mg/d per os (ASS-ratiopharm®; ratiopharm GmbH, Ulm, Germany) and dalteparin 5,000 IU/d subcutaneously (Fragmin®; Pfizer Pharma GmbH, Berlin, Germany).

INTRACARDIAC ECHOCARDIOGRAPHY, PRESSURE MEASUREMENTS AND CT

We performed ICE via the jugular vein using commercially available 8 or 10 Fr ultrasound catheters (AcuNav™; Siemens, Erlangen, Germany) and a Vivid q echo machine (GE Healthcare, Tirat Carmel, Israel). Measurements and classification of regurgitation and stenosis were carried out in accordance with international guidelines. The vena contracta, a semiquantitative measure for regurgitation, was expressed as a percentage of the inner diameter of the tissue-engineered conduit.

Invasive pressure measurements were conducted using a 5.2 Fr pigtail catheter connected to a monitor (Eagle 4000; Marquette Hellige, Freiburg, Germany).

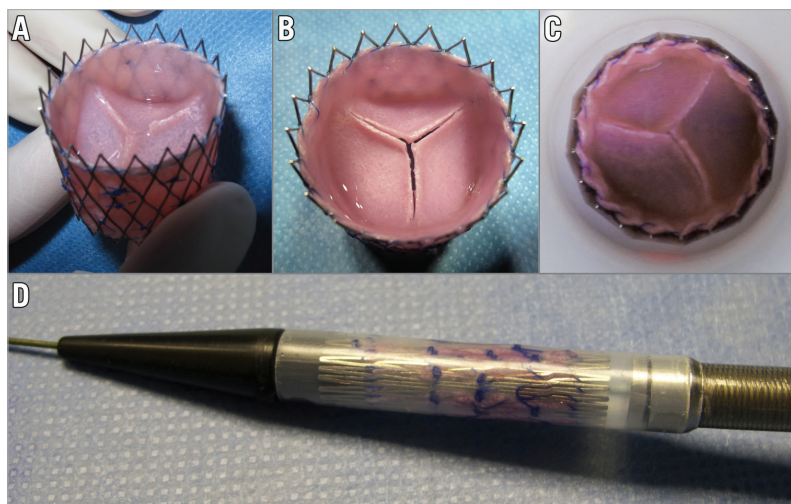


Figure 1. *sdTEHV and delivery system. At delivery, the leaflets were fused (A). After leaflet separation, a gap of up to 2 mm was present between the leaflets at full stent expansion to 30 mm (B). Crimping to 27 mm gave slight leaflet coaptation (C). The 26 Fr version of the delivery system, loaded with an sdTEHV (D).*

ECG-triggered flash CT scans (Somatom® Definition Flash; Siemens AG, Erlangen, Germany) with a slice thickness of 0.75 mm and contrast infusion of 2 to 2.5 ml/kg (Iomeron® 400 MCT; Bracco Imaging, Constance, Germany) were performed. Measurements were carried out with the syngo software (VE31H; Siemens AG).

A diastolic transverse section of the native pulmonary valve and the stent's mid portion were used to measure the minimal and maximal diameter as well as the circumference and area.

EXPLANTATION AND MACROSCOPIC EVALUATION OF THE sdTEHV

ICE, angiography and pressure measurements were repeated. An additional dose of heparin of 100 IU/kg was given. After sacrifice, the heart was explanted and the sdTEHV was dissected in one piece including the attached RVOT and PA.

(IMMUNO-) HISTOLOGY AND SCANNING ELECTRON MICROSCOPY (SEM)

These methods are described in the **Online Appendix**.

Statistics

Normal distribution of the data was assessed using histograms, QQ plots and the Shapiro-Wilks test. Values are expressed as mean±standard deviation. In the case of non-normally distributed data or sample sizes lower than 10, values are expressed as median and interquartile range. Non-parametric tests were performed. Related samples were tested using the Wilcoxon signed-rank test. Spearman's rank correlation coefficient was used to correlate the grade of insufficiency with the grade of stent ovality. Page's L test¹⁷ was applied to test whether the vena contracta increased during the follow-up. A p-value <0.05 was considered statistically significant.

Results

PERCUTANEOUS PULMONARY VALVE IMPLANTATION

The sheep had a mean weight of 47.3±5.8 kg and a mean pulmonary valve diameter of 24.6±2.5 mm.

The sdTEHV delivered to the catheterisation laboratory had homogeneous and smooth tissue. The leaflets were of equal

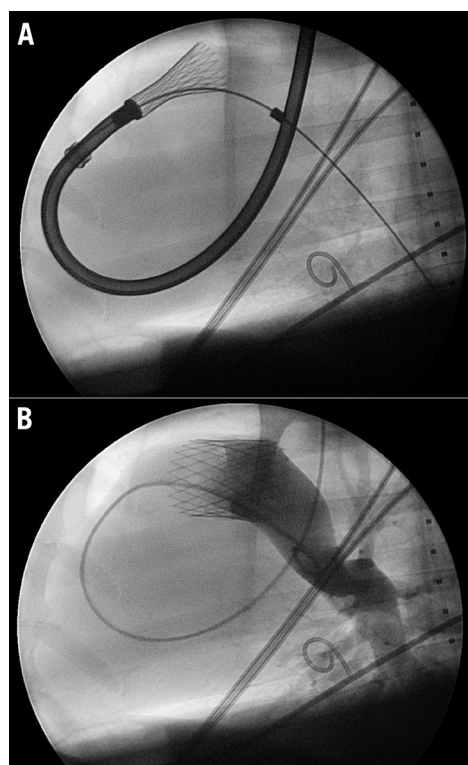


Figure 2. *Implantation. The jugular vein was used for implantation. The self-expanding stent was deployed by withdrawing the capsule and outer part of the shaft (both parts not visible under fluoroscopy) (A). The position and function of the sdTEHV was assessed by angiography (B).*

dimensions and concave with a curvature in circumferential but not in radial orientation (no hyperbolic shape). After separation, the leaflets slightly retracted leaving a gap of 1-2 mm between the margins. Coaptation was again achieved when the stent was crimped to 27 mm (**Figure 1**).

Crimping was successful in all but one valve, which was damaged during crimping; this valve was not implanted. In 10 animals the sdTEHV was loaded into an 8 mm capsule. In the five remaining animals a 10 mm capsule was used.

Implantation was successful in all 15 animals. All but one sdTEHV were successfully positioned over the native pulmonary valve. One sdTEHV was placed distally which resulted in a “double valve” with preserved native pulmonary valve closure. This valve was excluded from functional analysis.

Two valves were damaged during implantation. In one case a leaflet ruptured (confirmed at explantation) which resulted in immediate severe regurgitation. Possible mechanisms of damage include faulty crimping and withdrawing of the delivery system. In the other case the sdTEHV was creased during a first implantation attempt in which the capsule was accidentally detached from the shaft. This valve showed moderate regurgitation after successful implantation.

All animals completed the follow-up period as planned.

VALVE FUNCTION

The sdTEHV leaflets opened well following implantation. Stenosis did not occur at any point in time: ICE and invasive pressure measurements were unchanged compared to those before implantation ($p>0.05$) and all measurements stayed within the range of clinically normal values (**Table 1**, **Table 2**).

Immediately after implantation, there was no or only mild regurgitation in the majority of cases (eight of 14). Severe regurgitation occurred in two animals, one of which had a ruptured leaflet (mentioned above) while the other had severe oval stent deformation. Immediate regurgitation correlated with stent ovality assessed one week after implantation (Spearman's $\rho=0.64$) (**Figure 3**). At

week one the stents had expanded to near their maximal diameter. Stents did not significantly expand further during follow-up, but became more circular over time (**Table 3**).

During follow-up we noticed a continuous increase in non-coaptation, prolapse and significant shortening of the leaflets in all animals with a corresponding gradual increase in regurgitation grade and vena contracta ($p<0.01$) (**Figure 4**). Paravalvular leakage did not occur.

MACROSCOPIC FINDINGS

After eight weeks, broad stable adhesions between the tissue of the sdTEHV and the native PA and RVOT were present. The conduit and leaflets were overgrown by a thin layer of neointima. All valves were intact, except the one valve damaged during implantation. No large thrombi were seen.

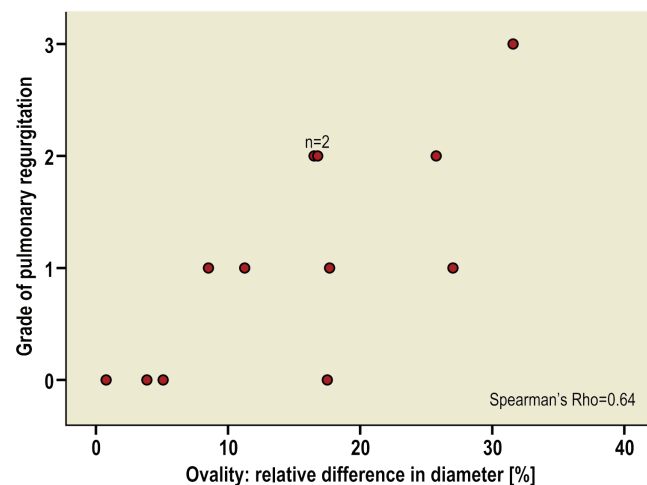


Figure 3. Correlation between stent ovality and regurgitation. The relative difference in diameter expresses the difference between the maximal and minimal diameter in relation to the mean diameter. Grades of pulmonary regurgitation: 0, trivial or none; 1, mild; 2, moderate; 3, severe.

Table 1. Systolic pressure gradient obtained by invasive pressure measurement.

Native pulmonary valve	sdTEHV after implantation	sdTEHV before explantation
6.6±2.7 mmHg	6.5±2.3 mmHg ^{ns}	7.9±6.3 mmHg ^{ns}

The pressure gradients of the sdTEHV at different time points were compared with those of the native pulmonary valve. ns: not significant

Table 2. Echocardiographic Doppler measurements of the native pulmonary valve and sdTEHV.

Follow-up, weeks	native (n=14)	0 (n=14)	4 (n=13)	8 (n=13)	12 (n=8)	16 (n=9)	20 (n=5)	24 (n=5)
Vmax, m/s	0.86 (0.30)	0.98 ^{ns} (0.40)	0.88 ^{ns} (0.40)	0.92 ^{ns} (0.50)	0.94 ^{ns} (0.30)	0.98 ^{ns} (0.50)	1.03 ^{ns} (0.40)	0.78 ^{ns} (0.70)
PGmax, mmHg	3.0 (1.8)	3.9 ^{ns} (3.1)	3.1 ^{ns} (2.9)	3.4 ^{ns} (4.0)	3.5 ^{ns} (2.2)	3.8 ^{ns} (3.8)	4.3* (3.6)	2.5 ^{ns} (5.2)
PGmean, mmHg	1.4 (0.8)	1.8 ^{ns} (1.6)	1.5 ^{ns} (1.2)	1.5 ^{ns} (1.5)	1.8 ^{ns} (1.2)	1.7 ^{ns} (1.7)	1.9 ^{ns} (1.6)	1.2 ^{ns} (2.3)

* $p<0.05$. Values are given as median with the interquartile range in brackets. The measurements obtained from the sdTEHV were compared with those of the native valve before implantation. n: number of animals; ns: not significant; PGmax: peak pressure gradient; PGmean: mean pressure gradient; Vmax: peak velocity

Table 3. Stent dimensions obtained from CT scans.

	Stent diameter	Stent ovality		
		Absolute diameter difference	Relative diameter difference	Ovality index
CT after implant	27.6±1.4 mm	3.9±2.8 mm	14.1±9.4%	1.16±0.11
CT before explant	27.9±1.0 mm	2.5±1.9 mm	8.9±6.8%	1.10±0.08
p-value	0.532	0.039	0.041	0.041

The difference between maximum and minimum diameter is given as absolute and relative difference (relative: percentage of the mean diameter). Ovality index: maximum diameter/minimum diameter. The CTs were performed 1.5±0.4 weeks after implantation and 1.3±0.7 weeks before explantation. In the CT before explantation, the diameter and ovality of the stent were equal among the different follow-up groups.

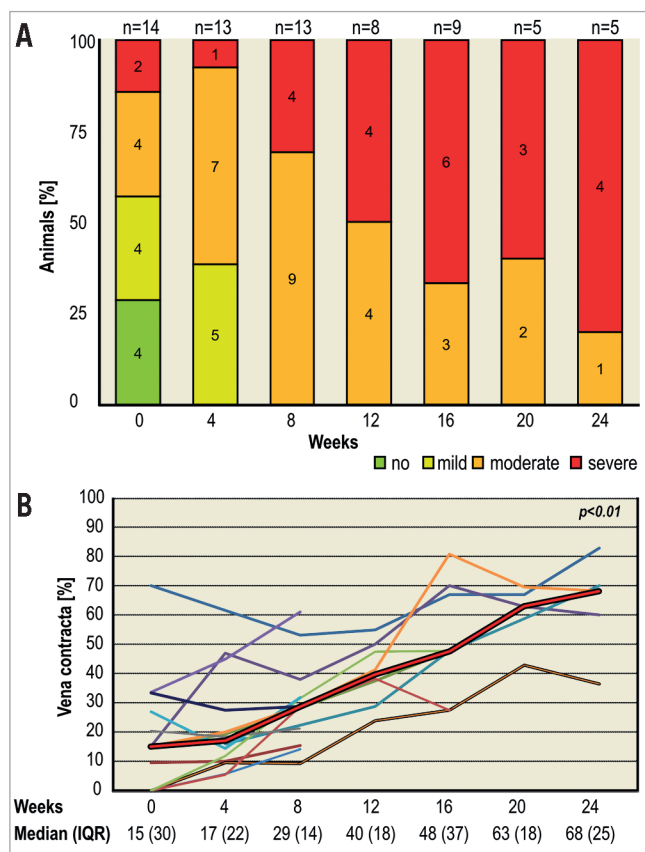


Figure 4. Progression of pulmonary regurgitation shown by echocardiography. Grade of pulmonary regurgitation (A): the numbers in the charts indicate the number of animals; one was excluded due to preserved native valve function. Three different sheep lacked one follow-up each. In the animals sacrificed at eight weeks, regurgitation was moderate in three and severe in two and at 16 weeks it was moderate in two and severe in three. Vena contracta (B): thin lines indicate individual animals. The bold red line represents the median. There was a significant increase of vena contracta over time ($p < 0.01$).

Leaflet shortening occurred in all animals in all follow-up groups. At eight weeks the commissural parts of the free leaflet margins still coapted. Leaflets were shortened at 16 weeks with a gap of several millimetres between the leaflets. At 24 weeks the leaflets were prolapsed and deformed with a wide central orifice (Figure 5).

Two factors contributing to leaflet shortening were observed: firstly, fusion of the leaflet with the conduit and secondly, leaflet retraction. Fusion of the hinge portion with the wall was the most obvious cause of leaflet shortening. It was more pronounced at 16 and 24 weeks than at eight weeks. Leaflet-wall fusion also occurred at the commissures, leading to a discontinuation of the intercommissural triangles after 24 weeks. Tissue retraction was seen at 16 weeks and had increased by 24 weeks (Figure 5).

MICROSCOPIC FINDINGS

In the non-implanted sdTEHV no cellular remnants were seen. The conduit and leaflet of this non-implanted valve were covered by a layer of collagenous ECM, with scattered remnants of scaffold throughout. This layer was most evident in the sinus of the valve. The hinge of the leaflet was fused with the wall for approximately 2 mm with a fine strip of ECM in between (Figure 6).

After eight weeks, the explanted sdTEHVs showed endothelialisation of all parts except the leaflet's ventricular surface and tip. After 16 weeks, the entire sdTEHV was covered by a confluent lining of endothelial cells (Figure 7).

Matrix host cell repopulation and remodelling were already seen after eight weeks. This process was first observed in the conduit wall, followed by the hinge area and finally the leaflet. Cells were identified as endothelial cells, macrophages, foreign body type cells, fibroblasts and lymphocytes.

After eight weeks, cells were found in highest densities in the wall and in lower densities in the hinge area and leaflet. After 16 and 24 weeks the density of cells in the leaflet and hinge area had increased while it had decreased again in the wall. In the wall, cells stained positive for α -SMA at eight weeks. In the leaflet, α -SMA positive cells were first found at 16 weeks and their number had increased by 24 weeks (Figure 8). Macrophages and foreign body giant cells were found next to the scaffold remnants in all cases. Scaffold material was progressively replaced by muscular matrix, but remnants remained at 24 weeks (Figure 6). Elastic fibres were detected in all explants with increasing density over time, starting in the wall, followed by detection in the hinge area after 16 weeks (Figure 8). No granulocytes were seen. Lymphocytes were homogeneously distributed all over the valve. Proportions of B-cells and T-cells were equal, as revealed by CD79 and CD3 staining (data not shown). Only one animal of the eight-week follow-up group

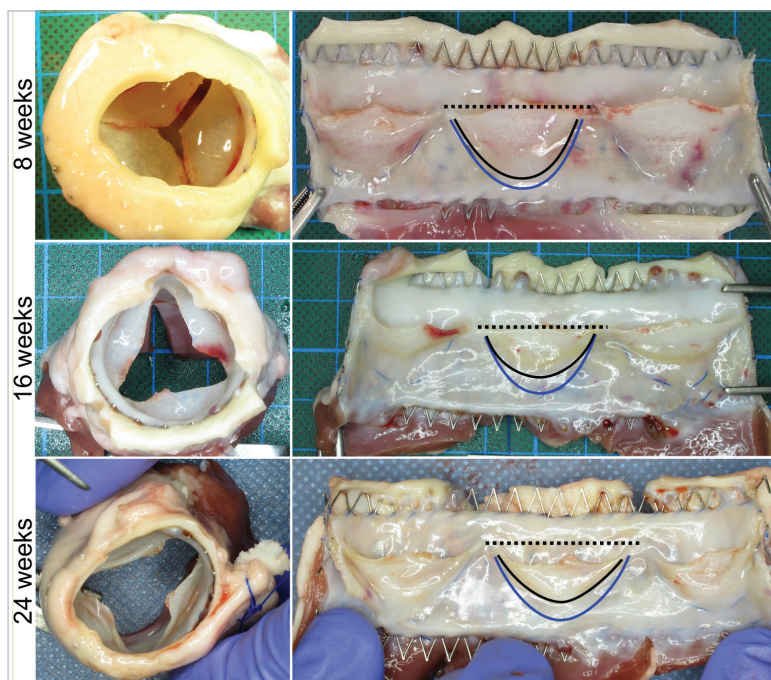


Figure 5. Macroscopic findings. The explanted valves had white and shiny homogeneous neo-tissue without any signs of intima hyperplasia, major thrombus formation, calcification or endocarditis. The leaflets progressively shortened, firstly due to a fusion of the leaflet bottom with the wall (blue line indicates the original position of the leaflet bottom and the black line the position of the leaflet bottom in the explanted valve) and secondly, due to tissue retraction (note the position of the free leaflet margin in relation to the black dashed line, which indicates the height of the commissures).

showed stronger infiltration of CD3-positive cells at the border between conduit and native wall.

Small thrombi were seen at the hinge point in five animals. These were covered by a fibromuscular matrix and were mainly seen in the short follow-up group (four at eight weeks, one at 24 weeks).

All other animals showed collagenous fibre formation in this area corresponding to the macroscopic fusion of leaflet and wall.

No calcification occurred in any of the sdTEHV, demonstrated by the absence of positive Von Kossa staining in all explanted valves (data not shown).

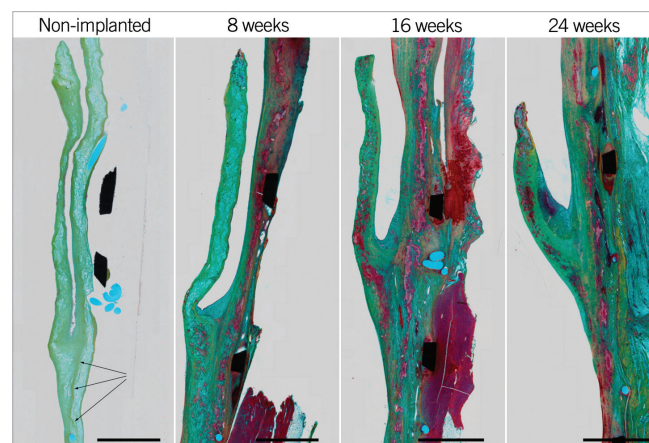


Figure 6. Extracellular matrix. Movat pentachrome staining of plastic embedded samples. In the non-implanted valve, scaffold remnants (light blue) are covered by collagenous ECM (light green) and approximately 2 mm of the bottom leaflet was fused to the wall (arrows). With time, scaffold remnants were replaced by muscular matrix (red) and the leaflet shortened due to retraction and leaflet-wall fusion. Scale bars represent 2 mm.

Discussion

The goal of the past two decades of heart valve tissue engineering has been to develop a heart valve replacement that replicates the native valve. This includes not only the appropriate physiological functions of opening and closing, but also the capability of the valvular tissue actively to maintain and repair itself. The recent development of an “off-the-shelf” tissue-engineered decellularised homologous valve, which after implantation is populated with the patient’s autologous cells, is a promising step towards attaining this goal.

Percutaneous xenogeneic valve replacement is now widespread in clinical practice in selected patients despite known chronic valve degeneration. For a population of younger patients with complex cardiac malformations requiring multiple cardiac interventions, xenogeneic valves can only be an interim solution. A percutaneous valve which does not degenerate is the ultimate aim.

This study represents a milestone in the development towards clinical application of both percutaneous valve replacement technology and tissue engineering. We successfully developed a tissue-engineered valve that can be taken “off-the-shelf” and that is implanted percutaneously and completely populated by the recipient’s cells *in vivo*.

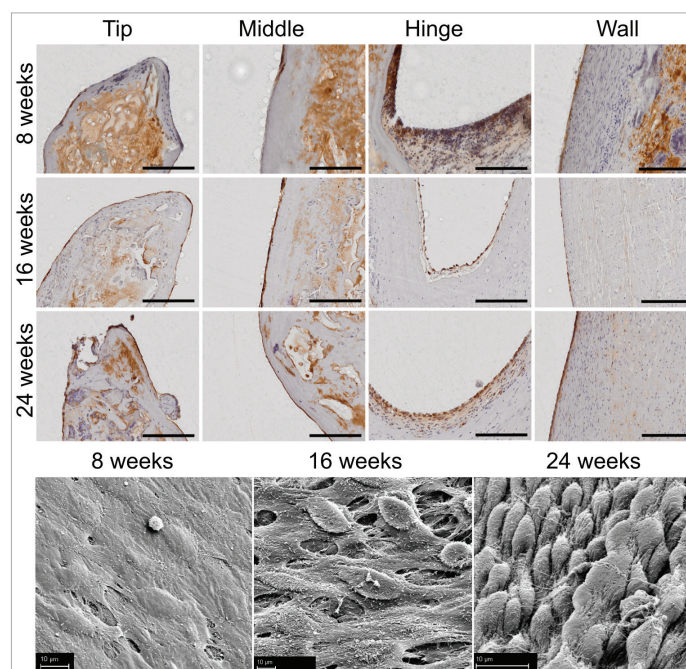


Figure 7. Endothelialisation. At 16 weeks the entire sdTEHV was covered by a confluent lining of endothelial cells. Von Willebrand factor staining of plastic-embedded samples (top), scale bars represent 200 μm . Scanning electron microscopy (bottom), scale bar represents 10 μm .

We achieved an acceptable crimping ratio of the valve, smaller than in a previous transapical study¹⁴ and comparable to that of early commercial systems for transfemoral pulmonary valve prostheses¹⁸. By size, a translation from jugular access in sheep to femoral access in humans seems feasible. Implantation was successful in all animals. Nevertheless, two valves were damaged during implantation due to initial delivery system problems, which were corrected during the course of the study.

The sdTEHV opened excellently with normal pressure gradients. However, immediate valvular regurgitation occurred in nearly half of the animals. Over time, all valves developed progressive regurgitation. Immediate and progressive valvular regurgitation was caused by several factors. In our opinion, the most important and central reason for regurgitation was the suboptimal valve design and the *in vitro* culture technique.

The problematical aspects of valve design were a lack of curvature in the radial orientation of the leaflets (no hyperbolic shape), a short coaptation zone and non-coaptation at full stent expansion. These design deficits resulted from the *in vitro* culture technique which was unable to preserve curved tissue shapes in the presence of cellular traction forces: the valves were cultured as living heart valves using myofibroblasts¹⁰. During culture, these cells exerted traction, causing shortening and compaction of the tissue unless a constraint was present¹². Although leaflets were fused at their free margins to prevent retraction¹⁰, there was no physical constraint to maintain a curved shape. Therefore, the leaflets flattened where possible, and neither a hyperbolic shape nor a longer coaptation zone was present.

Non-coaptation of the separated leaflets at full stent expansion was caused by different factors: firstly, the sdTEHVs were

cultured on an underexpanded stent to achieve self-anchorage in the bioreactor. Secondly, it was shown that, despite decellularisation, tissue will retract by 4% after the release of constraints (here leaflet separation) due to residual stress in the ECM¹². Finally, we noted that approximately 2 mm of the leaflet's bottom part was fused to the wall after culture. Leaflet coaptation was achieved only when the stent was not fully expanded in a circular shape. There was no leaflet reserve to compensate for oval deformation of the implanted valve. These findings underline the suboptimal preconditions of the sdTEHV for immediate function.

Progressive regurgitation occurred due to continuous shortening of the leaflets, while stent ovality became less over time. Leaflet shortening was mainly caused by fusion of the leaflet with the wall; leaflet retraction seemed to be an additional factor. In our opinion, fusion and retraction were promoted by the design deficits and the resulting regurgitation. These design deficits and consequent acute regurgitation might cause a non-physiologic blood flow pattern in diastole, and a decrease in load on the leaflets. This would reduce cell wash-out from the sinuses, promote fusion between leaflet and wall, and decrease load-induced leaflet straining. However, this strain is essential to counteract cellular traction forces to prevent cell-mediated leaflet retraction¹⁹. In accordance with other studies^{13,14}, ours demonstrated repopulation of the leaflets with contractile cells (α -SMA positive) at 16 weeks that had increased by 24 weeks. This corresponded with the macroscopic aspect of increasing leaflet retraction over time.

To achieve longevity of sdTEHVs, sufficient diastolic leaflet strain is mandatory for the remodelling process. Computational models showed that a longer coaptation zone, higher commissures and a hyperbolic shape would augment leaflet strain²⁰.

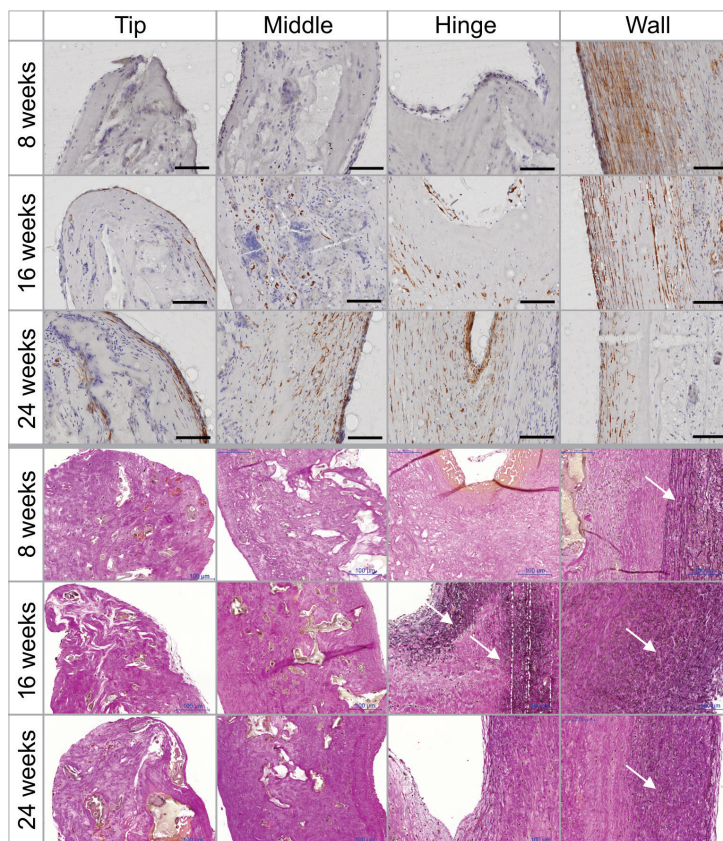


Figure 8. Cell population and remodelling of the matrix. The histological stainings showed an increase of cell infiltration and collagen formation over time. α -SMA staining of plastic-embedded samples (top). Elastica van Gieson staining of paraffin-embedded samples (bottom). Scale bars represent 100 μ m. White arrows indicate the presence of elastic fibres.

Optimisation of the design in terms of a more perpendicular angle of the hyperbolic-shaped leaflet in relation to the wall might also prevent leaflet-wall fusion as well as microscopic thrombi in the hinge area due to a more physiologic blood flow pattern with an adequate cell wash-out from the sinuses.

Despite these design deficits, the histologic results are promising, with complete endothelialisation of the valve and rapid autologous recellularisation and remodelling of the entire valvular matrix. As in other studies of sdTEHVs, no adverse reactions such as major thrombi, intimal hyperplasia, endocarditis, calcification or graft rejection were seen^{13,14}. Long-term animal studies are needed to prove that leaflet shortening can be prevented by design optimisation.

Limitations

A prototype was used. The *in vitro* culture technique needs to be refined to realise design optimisations in the presence of cellular traction forces. The sdTEHVs were implanted in healthy RVOTs. Cell repopulation from surrounding tissue may differ if the valve is implanted in a patient with previous pulmonary interventions.

Conclusions

Off-the-shelf sdTEHVs with a diameter of 30 mm can be implanted as pulmonary valve replacements using a 26 Fr delivery system in a percutaneous transvenous approach. The fast population with

autologous cells and the extensive matrix remodelling by these cells demonstrate the potential for matrix self-maintenance and longevity of the valve. Further design optimisation is required to prevent leaflet shortening and subsequent regurgitation.

Impact on daily practice

The concept of homologous tissue-engineered and decellularised off-the-shelf heart valves is a smart one to overcome the problem of tissue degeneration and the limited durability of today's percutaneous xenogeneic replacement valves. This new technology has the potential to become the next generation of percutaneous valve prosthesis because, firstly, this valve is a sterilisable, storable and non-immunogenic off-the-shelf bio-device which can be produced in all desired sizes. Secondly, it is thin, flexible and stable enough to be crimped and implanted via a percutaneous approach. Thirdly, the valve becomes a living autologous valve *in vivo* with the capacity to remodel and maintain its tissue, thus fulfilling the key criterion for longevity.

Acknowledgements

We thank our team members Katie Weber and Stefan Schröder for their tireless efforts concerning this project. We especially thank our veterinarians Fabienne Ferrara, Angela Körner and Kerstin

Brakmann for contributing to this project with their effort, skills and expertise. Olivier Levionnois (Switzerland) gave fruitful advice regarding the anaesthesia. We thank Carla Weber for post-editing, Julia Stein for statistical support and Anne Gale for editorial assistance (all DHZB). Further, the authors thank Ladina Ettinger (UZH) and the Centre for Microscopy and Image Analysis (UZH), especially Klaus Marquardt, for their excellent technical support.

Funding

This project was funded by the European Union's Seventh Framework Program, grant agreement number 242008 (LifeValve).

Conflict of interest statement

The authors have no conflicts of interest to declare.

References

1. Chaturvedi RR, Redington AN. Pulmonary regurgitation in congenital heart disease. *Heart*. 2007;93:880-9.
2. Cuypers JA, Witsenburg M, van der Linde D, Roos-Hesselink JW. Pulmonary stenosis: update on diagnosis and therapeutic options. *Heart*. 2013;99:339-47.
3. Ringewald JM, Suh EJ. Transcatheter pulmonary valve insertion: when, how, and why. *Cardiol Young*. 2012;22:696-701.
4. McElhinney DB, Hennesen JT. The Melody® valve and Ensemble® delivery system for transcatheter pulmonary valve replacement. *Ann N Y Acad Sci*. 2013;1291:77-85.
5. Kenny D, Hijazi ZM, Kar S, Rhodes J, Mullen M, Makkar R, Shirali G, Fogel M, Fahey J, Heitschmidt MG, Cain C. Percutaneous implantation of the Edwards SAPIEN transcatheter heart valve for conduit failure in the pulmonary position: early phase I results from an international multicenter clinical trial. *J Am Coll Cardiol*. 2011;58:2248-56.
6. Schoen FJ. Evolving concepts of cardiac valve dynamics: the continuum of development, functional structure, pathobiology, and tissue engineering. *Circulation*. 2008;118:1864-80.
7. Flanagan TC, Sachweh JS, Frese J, Schnöring H, Gronloh N, Koch S, Tolba RH, Schmitz-Rode T, Jockenhoewel S. In vivo remodeling and structural characterization of fibrin-based tissue-engineered heart valves in the adult sheep model. *Tissue Eng Part A*. 2009;15:2965-76.
8. Gottlieb D, Kunal T, Emani S, Aikawa E, Brown DW, Powell AJ, Nedder A, Engelmayr GC Jr, Melero-Martin JM, Sacks MS, Mayer JE Jr. In vivo monitoring of function of autologous engineered pulmonary valve. *J Thorac Cardiovasc Surg*. 2010;139:723-31.
9. Syedain ZH, Lahti MT, Johnson SL, Robinson PS, Ruth GR, Bianco RW, Tranquillo RT. Implantation of a Tissue-engineered Heart Valve from Human Fibroblasts Exhibiting Short Term Function in the Sheep Pulmonary Artery. *Cardiovasc Eng Technol*. 2011;2:101-112.
10. Dijkman PE, Driessen-Mol A, Frese L, Hoerstrup SP, Baaijens FP. Decellularised homologous tissue-engineered heart valves as off-the-shelf alternatives to xeno- and homografts. *Biomaterials*. 2012;33:4545-54.
11. Syedain ZH, Bradee AR, Kren S, Taylor DA, Tranquillo RT. Decellularised tissue-engineered heart valve leaflets with recellularisation potential. *Tissue Eng Part A*. 2013;19:759-69.
12. Van Vlimmeren MA, Driessen-Mol A, Oomens CW, Baaijens FP. Passive and active contributions to generated force and retraction in heart valve tissue engineering. *Biomech Model Mechanobiol*. 2012;11:1015-27.
13. Weber B, Dijkman PE, Scherman J, Sanders B, Emmert MY, Grünenfelder J, Verbeek R, Bracher M, Black M, Franz T, Kortsmits J, Modregger P, Peter S, Stampanoni M, Robert J, Kehl D, van Doeselaar M, Schweiger M, Brokopp CE, Wälchli T, Falk V, Zilla P, Driessen-Mol A, Baaijens FP, Hoerstrup SP. Off-the-shelf human decellularised tissue-engineered heart valves in a non-human primate model. *Biomaterials*. 2013;34:7269-80.
14. Driessen-Mol A, Emmert MY, Dijkman PE, Frese L, Sanders B, Weber B, Cesarovic N, Sidler M, Leenders J, Jenni R, Grünenfelder J, Falk V, Baaijens FP, Hoerstrup SP. Transcatheter implantation of homologous "off-the-shelf" tissue-engineered heart valves with self-repair capacity: long-term functionality and rapid in vivo remodeling in sheep. *J Am Coll Cardiol*. 2014;63:1320-9.
15. Bartosch M, Peters H, Spriestersbach H, O H-Ici D, Berger F, Schmitt B. A Universal Delivery System for Percutaneous Heart Valve Implantation. *Ann Biomed Eng*. 2016 Feb 10. [Epub ahead of print].
16. Mol A, Driessen NJ, Rutten MC, Hoerstrup SP, Bouten CV, Baaijens FP. Tissue engineering of human heart valve leaflets: a novel bioreactor for a strain-based conditioning approach. *Ann Biomed Eng*. 2005;33:1778-88.
17. Page E. Ordered hypotheses for multiple treatments: a significance test for linear ranks. *J Am Stat Assoc*. 1963;58:216-30.
18. Ewert P, Horlick E, Berger F. First implantation of the CE-marked transcatheter Sapien pulmonic valve in Europe. *Clin Res Cardiol*. 2011;100:85-7.
19. Van Loosdregt IA, Argento G, Driessen-Mol A, Oomens CW, Baaijens FP. Cell-mediated retraction versus hemodynamic loading - A delicate balance in tissue-engineered heart valves. *J Biomech*. 2014;47:2064-9.
20. Loerakker S, Argento G, Oomens CW, Baaijens FP. Effects of valve geometry and tissue anisotropy on the radial stretch and coaptation area of tissue-engineered heart valves. *J Biomech*. 2013;46:1792-800.
21. Quentin T, Poppe A, Bär K, Sigler A, Foth R, Michel-Behnke I, Paul T, Sigler M. A novel method for processing resin-embedded specimens with metal implants for immunohistochemical labelling. *Acta Histochem*. 2009;111:538-42.

Supplementary data

Online Appendix. Histological methods.

Online Table 1. Antibodies for immunohistochemical staining of plastic-embedded samples.

The supplementary data are published online at:
http://www.pconline.com/eurointervention/98th_issue/12



Supplementary data

Online Appendix. Histological methods

PLASTIC EMBEDDING

A block containing half of an sdTEHV leaflet, attached stent and surrounding native tissue was cut and fixed in formalin. The specimen was embedded in methylmethacrylate (Technovit® 9100; Kulzer & Co, Wehrheim, Germany), sectioned in slices of 0.5 mm using a diamond cutter (300 CP; EXAKT GmbH, Norderstedt, Germany) and ground to 10-30 µm using a rotational grinder (400 CS; EXAKT GmbH). Standard staining was performed using Richardson blue. For immunohistochemical staining, deplastification was performed²¹. Binding of primary antibodies was detected using horseradish peroxidase-conjugated secondary antibodies. The sections were counterstained with hemalaun. As primary antibodies, we used anti-smooth muscle actin (SMA) to detect α -SMA positive cells, von Willebrand Factor for endothelial cells, CD3 for T-lymphocytes and CD79 for B-lymphocytes (**Online Table 1**). Deplastification was performed for implementation of Movat pentachrome staining (identification of ECM components). An unimplanted valve served as a control.

CONVENTIONAL HISTOLOGY

Another half of a leaflet was detached from stent and native tissue. Subsequently, it was embedded in paraffin and cut into 7 µm

sections. These sections were stained with haematoxylin and eosin to visualise general tissue morphology and to identify the presence of cells. Further, Verhoeff-Van Gieson staining was performed to visualise collagen and elastic fibres and von Kossa staining to detect calcification. To assess the phenotype of the infiltrated cells in the explanted leaflets and to assess endothelialisation of the valvular surface, immunohistology was performed using the Ventana BenchMark automated staining system (Ventana Medical Systems, Tucson, AZ, USA) and antibodies for α -smooth muscle actin (α -SMA, clone 1A4; Sigma-Aldrich, St. Louis, MO, USA), vimentin (clone Vim 3B4; DakoCytomation, Copenhagen, Denmark) and CD31 (ab28364; Abcam, Cambridge, United Kingdom). Primary antibodies were detected with the Ventana iVIEW DAB detection kit, yielding a brown reaction product. All stainings were analysed by normal light microscopy.

SEM

In addition, representative tissue samples of both control and explanted decellularised TEHV were fixed in 2% glutaraldehyde (Sigma-Aldrich), platinum-sputtered and subsequently analysed by scanning electron microscopy (SEM) to assess valvular surface morphology.

Online Table 1. Antibodies for immunohistochemical staining of plastic-embedded samples.

Primary antibody	Dilution	Antigen retrieval	Secondary antibody	Target
Mouse anti-human smooth muscle actin, clone 1A4 (Dako)	1:50	Citrate buffer, pH 6, 40 min in a steamer	Rabbit anti-mouse immunoglobulin antibody (Dako), diluted 1:100	Smooth muscle cells
Polyclonal rabbit anti-human von Willebrand Factor (Dako)	1:400	Citrate buffer, pH 6, 40 min in a steamer	Swine anti-rabbit immunoglobulin antibody (Dako), diluted 1:100	Endothelial cells
Polyclonal rabbit anti-human CD3 (Dako)	1:100	Citrate pH 6 (Dako), 40 min in a steamer	Polyclonal rabbit anti-goat immunoglobulin/ horseradish peroxidase (Dako), diluted 1:100	T-lymphocytes
Monoclonal mouse anti-human CD79 α , clone HM57 (Dako)	1:100	Tris/ EDTA, pH 9, 20 min in a steamer	Rabbit anti-mouse immunoglobulin (Dako), diluted 1:100	B-lymphocytes